Thermochimica Acta 499 (2010) 48–53

Contents lists available at ScienceDirect

Thermochimica Acta

journal homepage: www.elsevier.com/locate/tca

$In_2Mo_3O_{12}$: A low negative thermal expansion compound

Bojan A. Marinkovic[a,*], Monica Ari[a], Paula Mendes Jardim[a], Roberto R. de Avillez[a], Fernando Rizzo[a], Fabio Furlan Ferreira[b]

[a] Departamento de Engenharia de Materiais, Pontifícia Universidade Católica de Rio de Janeiro – PUC-Rio, Rua Marquês de São Vicente 225, 22453-900 Gávea, RJ, Brazil
[b] Laboratório Nacional de Luz Síncrotron (LNLS), CP 6192, CEP 13083-970, Campinas, SP, Brazil

ARTICLE INFO

Article history:
Received 27 February 2009
Received in revised form 19 October 2009
Accepted 31 October 2009
Available online 10 November 2009

Keywords:
Thermal expansion
X-ray diffraction
Phase transition
Molibdates
Catalyst

ABSTRACT

Orthorhombic $In_2Mo_3O_{12}$ has low negative linear coefficient of thermal expansion ($\alpha_l = -1.85 \times 10^{-6}\,^{\circ}C^{-1}$) as evaluated by X-ray powder diffraction using a synchrotron facility. The linear coefficient of thermal expansion for orthorhombic $In_2Mo_3O_{12}$ is directly dependent on the inherent volume distortion parameter (υ) of InO_6. This finding strongly corroborates the recently proposed relationship between the linear coefficient of thermal expansion in $A_2M_3O_{12}$ compounds (α_l) and the distortion level of AO_6 polyhedra. With the increase of inherent distortion parameter (υ) of AO_6 polyhedra, the linear coefficient of thermal expansion becomes more negative. Another important feature of AO_6 polyhedra, including InO_6, is that their distortion increases as a function of temperature. Orthorhombic $In_2Mo_3O_{12}$ is stable in the studied temperature range, 370–760 °C.

1. Introduction

In accordance to some recent findings, $In_2Mo_3O_{12}$ compound is an outstanding catalyst for the production of olefin from paraffin [paraffin = olefin + hydrogen] through dehydrogenation (DH) followed with selective hydrogen combustion (SHC) in a process which is not thermodynamically restricted [1]. It is suggested that in this process, operating in the temperature range between 450 °C and 550 °C, $In_2Mo_3O_{12}$ compound oxidizes with great preference H_2 in comparison to olefins (propylene) showing high selectivity of almost 99%. However, there is lack of information in literature about the thermal properties of this compound, such as thermal expansion coefficient and thermal structure stability. It is only known that this one presents a first order phase transition at around 335 °C to 337 °C, from monoclinic to orthorhombic structure as determined by thermal methods [2,3], while a recent thermochemical study pointed out that the orthorhombic phase is entropically stabilized since it has positive enthalpy of formation [3].

Since Evans et al. [4] pioneering work on the thermal expansion of some molybdates and tungstates from $A_2M_3O_{12}$ family, where *A* could be any trivalent transition metal and/or rare earth element, while *M* is generally some hexavalent cation such as Mo^{6+} or W^{6+}, it is generally established that monoclinic phases show normal (positive) thermal expansion coefficients, while orthorhombic modifications demonstrate negative thermal expansion (NTE), although there are several exceptions from this rule [5]. Marinkovic et al. have systematically studied $A_2M_3O_{12}$ and structurally related families [5–8] due to their high chemical flexibility and, therefore, due to the possibility of synthesis of new materials with controlled thermal expansion coefficients. Very recently, they proposed [8] that the linear coefficient of thermal expansion (α_l) of the $A_2M_3O_{12}$ compounds is directly dependent on the distortion level of AO_6 polyhedra. This polyhedral distortion is expressed through the *inherent volume distortion parameter* (υ) – defined as the distortion of AO_6 polyhedra at the lowest available temperature – as suggested by Marinkovic et al. [8], based on the polyhedra distortion parameter originally introduced by Makovicky and Balic-Zunic [9]. In another study of considerable interest for understanding of $A_2M_3O_{12}$ compounds, Hu et al. studied the influence of light and heavy rare earth elements on its thermal expansion properties [10].

Herewith, we report our findings on the thermal expansion and structure stability of $In_2Mo_3O_{12}$, a member of $A_2M_3O_{12}$ family not previously characterized for these properties as far as the authors are aware of. A detailed understanding of thermal expansion properties of $A_2M_3O_{12}$ family is fundamental for eventual future applications of these phases in composites, substrates for high-precision optical applications and/or Fiber Bragg gratings. However, several issues essential for application of this family in practical purposes are not well understood.

First, engineering of controllable thermal expansion materials (solid solutions) is still not well resolved. For example, it was unexpectedly found that $AlFeMo_3O_{12}$ and $Al_{1.4}Fe_{0.6}Mo_3O_{12}$ phases in $Al_{2-x}Fe_xMo_3O_{12}$ system have higher positive linear coefficients of thermal expansion (α_l) than the pure phases

* Corresponding author. Tel.: +55 21 3547 1954; fax: +55 21 3547 1248.
E-mail address: bojan@puc-rio.br (B.A. Marinkovic).

0040-6031/$ – see front matter © 2009 Elsevier B.V. All rights reserved.
doi:10.1016/j.tca.2009.10.021

($Al_2Mo_3O_{12}$ and $Fe_2Mo_3O_{12}$) [5]. Linear coefficients of thermal expansion in $Cr_{2-x}Fe_xMo_3O_{12}$, $Y_{2-x}Nd_xW_3O_{12}$, $Y_{2-x}Sm_xW_3O_{12}$ and $Cr_{2-x}Yb_xMo_3O_{12}$ solid solutions [5,11–13] also deviate from the expected trend which assumes that negative thermal expansion will become more negative with the entrance of larger A^{3+} in the structure of $A_2M_3O_{12}$ phases [14].

Secondly, in accordance to this classical and reasonable rationalization NTE becomes more negative with increase of A^{3+} radius which enhances slight polyhedra shape changes as a function of the temperature required for the appearance of rocking motions in this structural family [14]. Therefore, considering In^{3+} radius of 0.80 Å, $In_2Mo_3O_{12}$ should demonstrate a negative thermal expansion coefficient higher than the measured for $Sc_2Mo_3O_{12}$ ($\alpha_l = -2.1 \times 10^{-6}\,^{\circ}C^{-1}$) [15], but lower than the evaluated for $Lu_2W_3O_{12}$ ($\alpha_l = -6.8 \times 10^{-6}\,^{\circ}C^{-1}$) [14] (see also Fig. 5 in Ref. [5] for the complete picture of this dependence). However, there are already several examples of discrepancy between the expected and measured values of linear coefficients of thermal expansion, such as $Cr_2Mo_3O_{12}$, $Fe_2Mo_3O_{12}$ [5], $Tm_2Mo_3O_{12}$ and $Tm_2W_3O_{12}$ [16].

At last, the factors that control the temperature of phase transition between monoclinic and orthorhombic phases (with generally negative thermal expansion although several exceptions show positive expansion) are also not fully understood [8]. Therefore, having this in mind it can be inferred that there is still lot of room for further investigation of these materials.

This study has two additional aims. In order to evaluate the robustness of the previously proposed dependence between the distortion level of AO_6 polyhedra and the linear coefficient of thermal expansion (α_l) [8], it is necessary to test other $A_2M_3O_{12}$ compounds that have not been previously evaluated due to the lack of crystal structure data (and their variations with temperature). Also, $In_2Mo_3O_{12}$ is potentially attractive for catalytic purposes, operating in the temperature range from 450 °C to 550 °C, therefore, it is necessary to evaluate its thermal properties.

2. Experimental

$In_2Mo_3O_{12}$ was produced by solid-state reaction from a stoichiometric mixture of MoO_3 (Fluka 99.98%) and In_2O_3 (Fluka 99.9%). The reactants were preheated at 500 °C for three hours, then weighed, mixed and homogenized in agate mortar. The preheated powders were heat treated in alumina crucibles at 700 °C for 48 h, followed by an intermediate grinding at room temperature, heated again at 780 °C for 20 h and cooled down in furnace.

High-temperature X-ray powder diffraction (HTXRPD) was collected in air at seven different temperatures (100 °C, 200 °C, 320 °C, 370 °C, 500 °C, 630 °C and 760 °C) at the X-ray Powder Diffraction (D10B-XPD) beamline [17] of the Brazilian Synchrotron Light Laboratory (LNLS). The samples were placed after a dipolar source. X-rays of wavelength 1.23989 Å were selected by a double-bounce Si (1 1 1) monochromator, with water-refrigeration in the first crystal, while the second one is bent for sagittal focusing. The beam is vertically focused or collimated by a bent Rh-coated ultra low expansion glass mirror placed before the monochromator, which also provides filtering of high-energy photons (third- and higher-order harmonics). The vertically focused beam provided a spot of $\sim 1.0 \times 10^{-3}$ m (vertical) $\times \sim 2 \times 10^{-3}$ m (horizontal) into the sample position. The experiments were performed in the vertical scattering plane, i.e., perpendicular to the linear polarization of the incident photons. Wavelength and the zero point were determined from eleven well-defined reflections of the SRM640c silicon standard. The diffracted beam was analyzed with a Ge (1 1 1) crystal analyzer and detected with a Na(Tl)I scintillation counter with a pulse-height discriminator in the counting chain. The incoming beam was also monitored by a scintillation counter for normalization of the decay of the primary beam. The powder sample was measured in flat-plate geometry and data were recorded at different temperatures for ~0.5 s at each 2θ in steps of 0.003° from 10° to 70°. A calibration curve [5] for the furnace was obtained using a NIST Si sample and its cell parameter variation with temperature, provided by Yim and Paff [18].

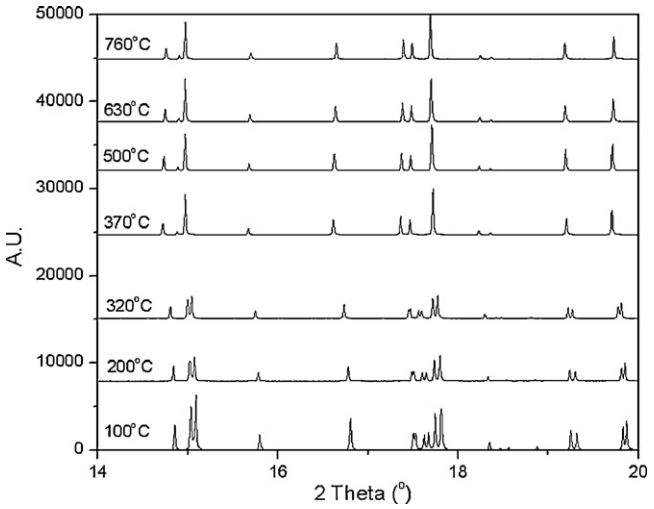

Fig. 1. High-resolution XRPD patterns for $In_2Mo_3O_{12}$ at 100, 200, 320 °C [monoclinic structure] and 370, 500, 630, 760 °C [orthorhombic structure].

LeBail and Rietveld (anisotropic) refinements were performed using Topas-Academic software [19]. Rietveld refinements of the orthorhombic structure were carried out in the standard space group Pbcn (no. 60) using, at the beginning, $Cr_2Mo_3O_{12}$ atomic positions (ICSD-418845) as the structural model. Analyses of InO_6 polyhedral distortion in orthorhombic structure at different temperatures were carried out by IVTON program [9].

3. Results

3.1. Phase transition and thermal expansion coefficients

X-ray powder diffraction (XRPD) data corroborated the existence of the phase transition between 320 °C and 370 °C (Fig. 1), previously observed by thermal methods at ~335–337 °C [2,3], showing that the low-temperature and high-temperature phases are monoclinic and orthorhombic, respectively, as confirmed through LeBail and Rietveld refinements of X-ray diffraction patterns (Fig. 2). Considering the unit-cell volumes calculated at 320 °C and 370 °C for monoclinic and orthorhombic phases, respectively, $\Delta V/Z$ (volume difference per chemical formula) on the phase transition is determined to be 4.38 Å^3 (+1.62%). This value of $\Delta V/Z$ for $In_2Mo_3O_{12}$ compares with $\Delta V/Z$ estimated for $Al_2Mo_3O_{12}$ and $Al_2W_3O_{12}$ [3].

The quality of the XRPD data acquired for the monoclinic phase in the temperature between 100 °C and 320 °C were not enough to permit Rietveld crystal structure outputs with physical merit as judged through the values of R_{Bragg} factors [20] (Table 1).

Table 1
Rietveld reliability factors for the refined diffraction patterns of $In_2Mo_3O_{12}$.

Temperature (°C)	R_{Bragg} (%)	Gof	R_{wp} (%)	R_{exp} (%)
100	6.44	1.82	17.32	9.53
200	5.98	1.42	20.72	13.46
320	10.98	1.99	27.32	13.75
370	5.43	1.59	22.37	14.12
500	6.29	1.71	23.52	13.73
630	6.76	1.81	26.10	14.43
760	5.88	1.69	24.02	14.25

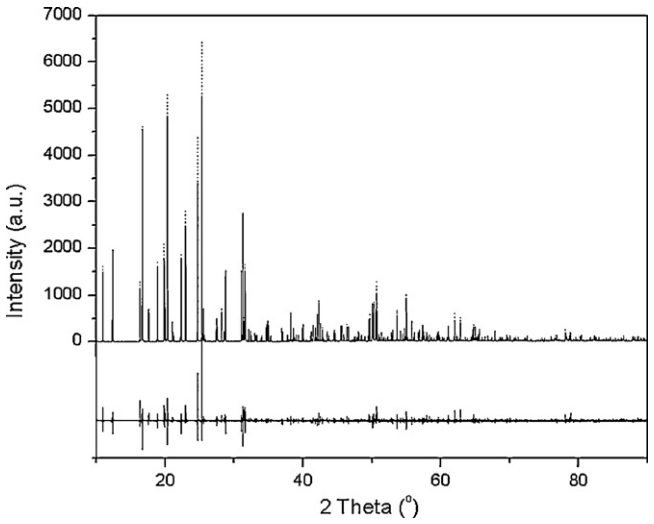

Fig. 2. High-resolution XRPD pattern for $In_2Mo_3O_{12}$ at 370 °C. Experimental profile (dot lines), calculated and difference profile (full lines).

Axial and linear thermal expansion coefficients (α_l) of monoclinic $In_2Mo_3O_{12}$ have been calculated using natural logarithmic plots (Fig. 3) through linear regression (with R values superior to 99%). Fig. 3 illustrates that all three unit-cell axes (a, b and c) demonstrated normal, positive, thermal expansion in the investigated temperature range, 100–320 °C. As-calculated α_l is highly positive $\alpha_l = 1.24 \times 10^{-5}\,°C^{-1}$, being higher than the α_l ($7.3 \times 10^{-6}\,°C^{-1}$) determined for monoclinic $Sc_2Mo_3O_{12}$ (4–178 K) [14].

Unit-cell parameters for the orthorhombic modification of $In_2Mo_3O_{12}$ have been calculated by Rietveld method. Fig. 4 summarizes the evaluation of axial and linear thermal expansion coefficients for this phase (R values were always superior to 99%). It is important to observe that the unit-cell axis a showed positive coefficient of thermal expansion ($\alpha_a = 5.46 \times 10^{-6}\,°C^{-1}$), differently from the axes b and c that both shrink with increase of temperature, their coefficients of thermal expansion being $-4.43 \times 10^{-6}\,°C^{-1}$ and $-6.41 \times 10^{-6}\,°C^{-1}$, respectively. These axial thermal expansion properties resulted in a low negative linear coefficient of thermal expansion of $-1.85 \times 10^{-6}\,°C^{-1}$. The coefficients of thermal expansion for both phases are summarized in Table 2.

3.2. Crystal structure of orthorhombic $In_2Mo_3O_{12}$

Rietveld refinement of orthorhombic $In_2Mo_3O_{12}$ was performed for XRPD patterns from 370 °C to 760 °C in order to evaluate temperature dependence of the crystal structure details, such as apparent bond lengths In–O and Mo–O, non-bonding distances In–Mo and interpolyhedral angles In–O–Mo. R_{Bragg} factors of $In_2Mo_3O_{12}$ for all temperatures are present in Table 1. This factor is higher for the XRPD at 630 °C than for the other three XRPD and, therefore, crystal structure output for 630 °C was not considered for discussion. The main obstacle to perform a better adjustment of XRPD in the range between 370 °C and 760 °C, comparing to some previous refinements [5,8], was the presence of very high texture along the [1 0 0] direction observed in this sample, a consequence of a pseudo two-dimensional crystal structure of $A_2M_3O_{12}$ family [21]. Fig. 5 exhibits a resume of the temperature dependence of the principal crystal structure parameters, generally associated

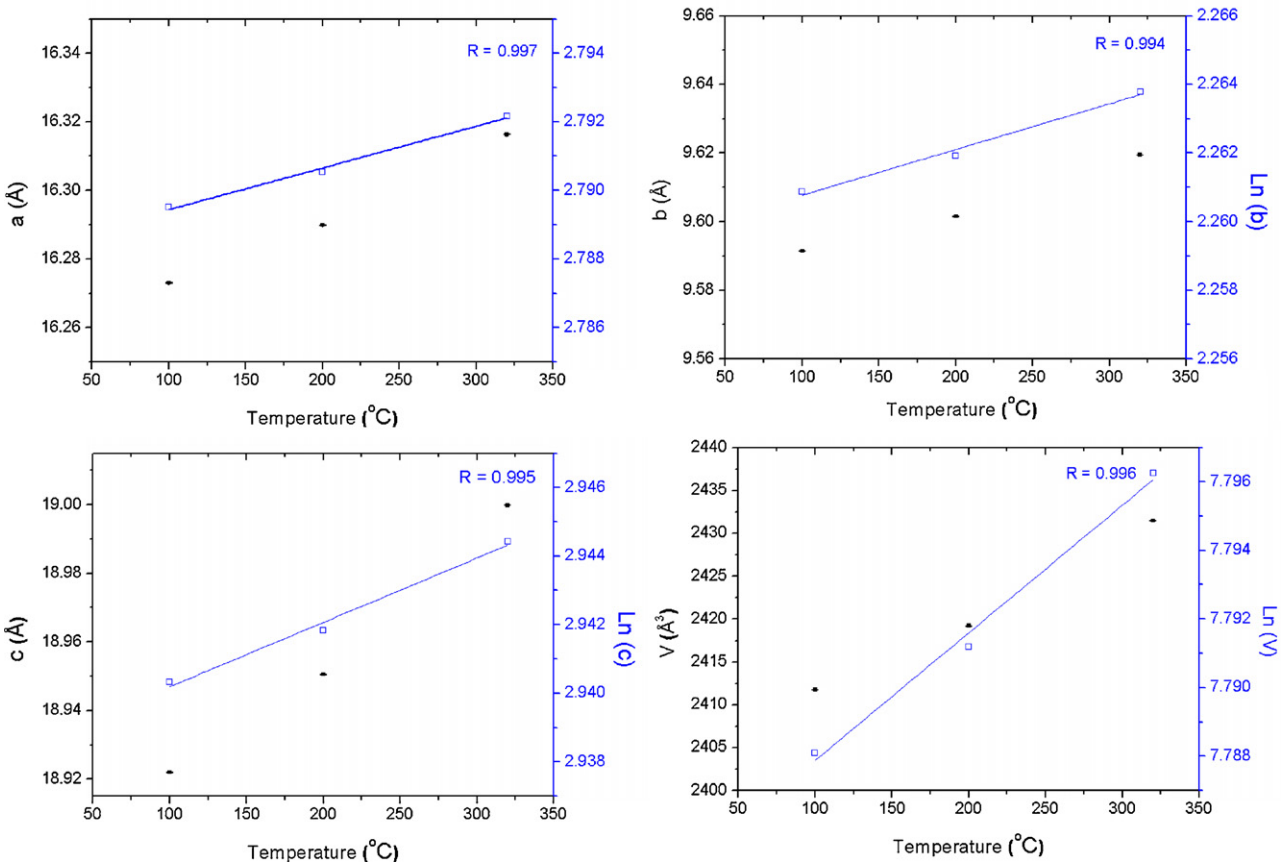

Fig. 3. Linear and natural logarithmic variations of cell parameters (a, b and c) and cell volume with temperature in the monoclinic structure, $P2_1/a$ space group. The linear regression of natural logarithmic plots (respective R values appear in each plot) was used for calculation of coefficients of thermal expansion. Standard uncertainties are included, but are too small to appear in the graphs.

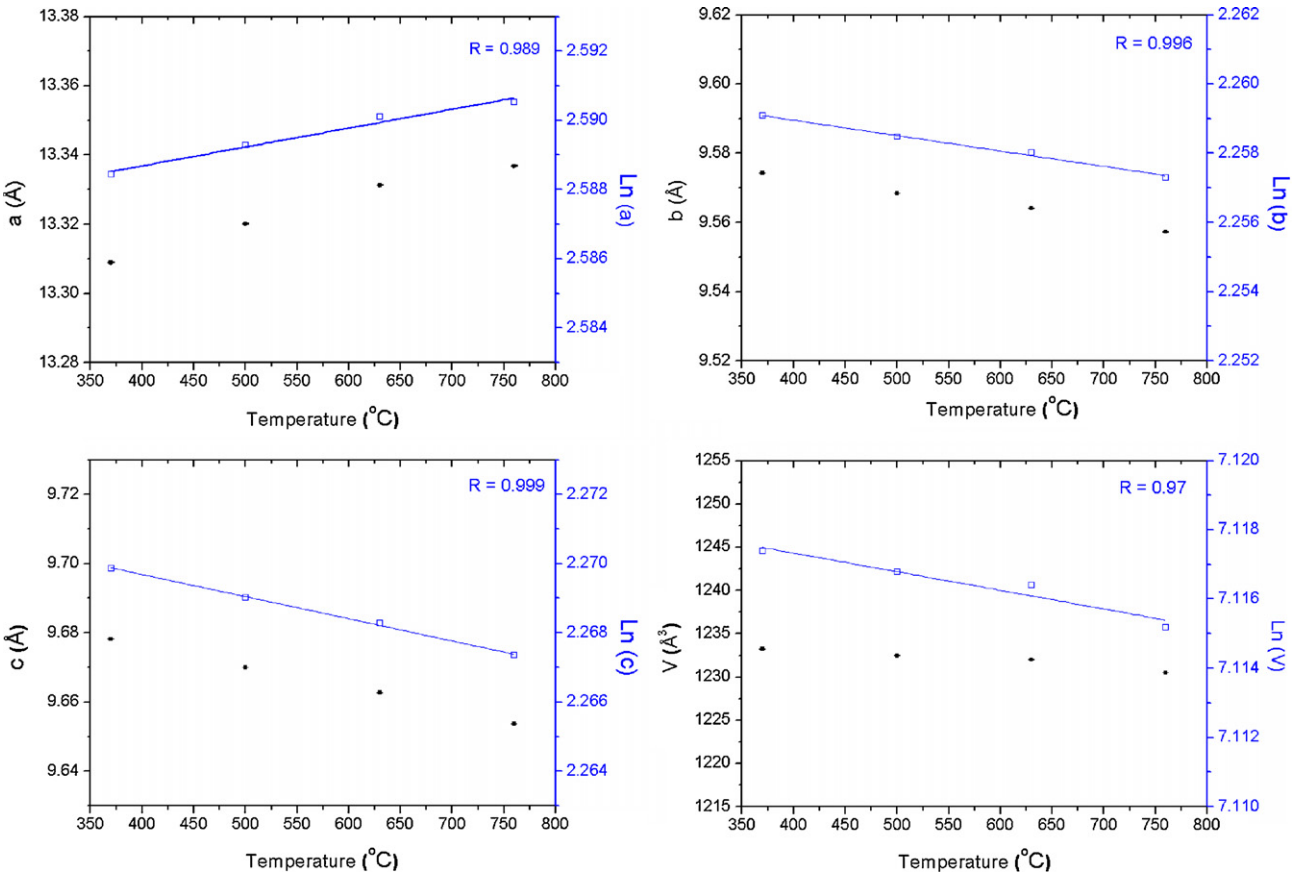

Fig. 4. Linear and natural logarithmic variations of cell parameters (a, b and c) and cell volume with temperature in the orthorhombic structure, Pbcn space group. The linear regression of natural logarithmic plots (respective *R* values appear in each plot) was used for calculation of coefficients of thermal expansion. Standard uncertainties are included, but are too small to appear in the graphs.

Table 2
Thermal expansion coefficients (α) of $In_2Mo_3O_{12}$ in the monoclinic and orthorhombic structure.

Structure	α			
	α_a [$\times 10^{-6}\,^\circ C^{-1}$]	α_b [$\times 10^{-6}\,^\circ C^{-1}$]	α_c [$\times 10^{-6}\,^\circ C^{-1}$]	α_l [$\times 10^{-6}\,^\circ C^{-1}$]
Monoclinic	12.1	13.3	18.8	12.4
Orthorhombic	5.46	−4.43	−6.41	−1.85

with the occurrence of NTE in $A_2M_3O_{12}$ compounds. In–Mo mean non-bonding distances and Mo–O mean apparent bond lengths were hardly reduced over the investigated temperature interval. In–O mean apparent bond length and mean In–O–Mo bond angles were the most affected structural parameters. Atomic positions and atomic displacement parameters for the temperatures of 370 °C, 500 °C and 760 °C are supplied in Supplementary information file.

4. Discussion

Orthorhombic $In_2Mo_3O_{12}$ shows positive thermal expansion along *a* axis, a characteristic of $A_2M_3O_{12}$ compounds that has been already observed, for example, in $Fe_{2-x}Cr_xMo_3O_{12}$, $Cr_{2-x}Al_xMo_3O_{12}$ and $Al_{2-x}Fe_xMo_3O_{12}$ solid solutions [6]. For these solid solutions, as well as for $In_2Mo_3O_{12}$, this characteristic is noticed over the whole investigated temperature range, while in $Y_2W_3O_{12}$ [22] and $Y_2Mo_3O_{12}$ [8] this axis changes its thermal expansion from positive to negative at near room temperatures. Regarding to its low negative linear coefficient of thermal expansion ($\alpha_l = -1.85 \times 10^{-6}\,^\circ C^{-1}$), it seems that $In_2Mo_3O_{12}$ represents another case of discrepancy [5] from the earlier proposed relationship that correlates linear coefficient of thermal expansion with the radii of A^{3+} cation [14]. Ari et al. have already pointed out several other compounds that do not strictly follow this relationship [5].

Based on the atomic positions of $In_2Mo_3O_{12}$ (see Supplementary information) one can calculate, using IVTON program, the inherent volume distortion parameter (υ) of InO_6 polyhedron and its variation as a function of temperature. Fig. 6 exhibits the relationship between linear coefficients of thermal expansion and inherent volume distortion parameter (υ) [8] for different compounds of $A_2M_3O_{12}$ family. This correlation shows a linear dependence between the thermal expansion and the inherent volume distortion parameter for all considered compounds. Apparently, this correlation shows a reasonable robustness (Fig. 6) still evidencing that υ in InO_6 (in $In_2Mo_3O_{12}$) and ScO_6 (in $Sc_2W_3O_{12}$) are similar, although α_l of $Sc_2Mo_3O_{12}$ is *ca.* 15% more negative than α_l of $In_2Mo_3O_{12}$. Volume distortion parameter of InO_6 increases with temperature from 0.12% at 370 °C and 0.14% at 500 °C to 0.18% at 760 °C. The increase of distortions in AO_6 polyhedra as a function of temperature was previously verified for all other studied phases of $A_2M_3O_{12}$ [8].

Orthorhombic $In_2Mo_3O_{12}$ is stable in air in the temperature interval considered for catalytic purposes (450–550 °C) [1] and, at least, until 760 °C. In the operating temperature interval it has

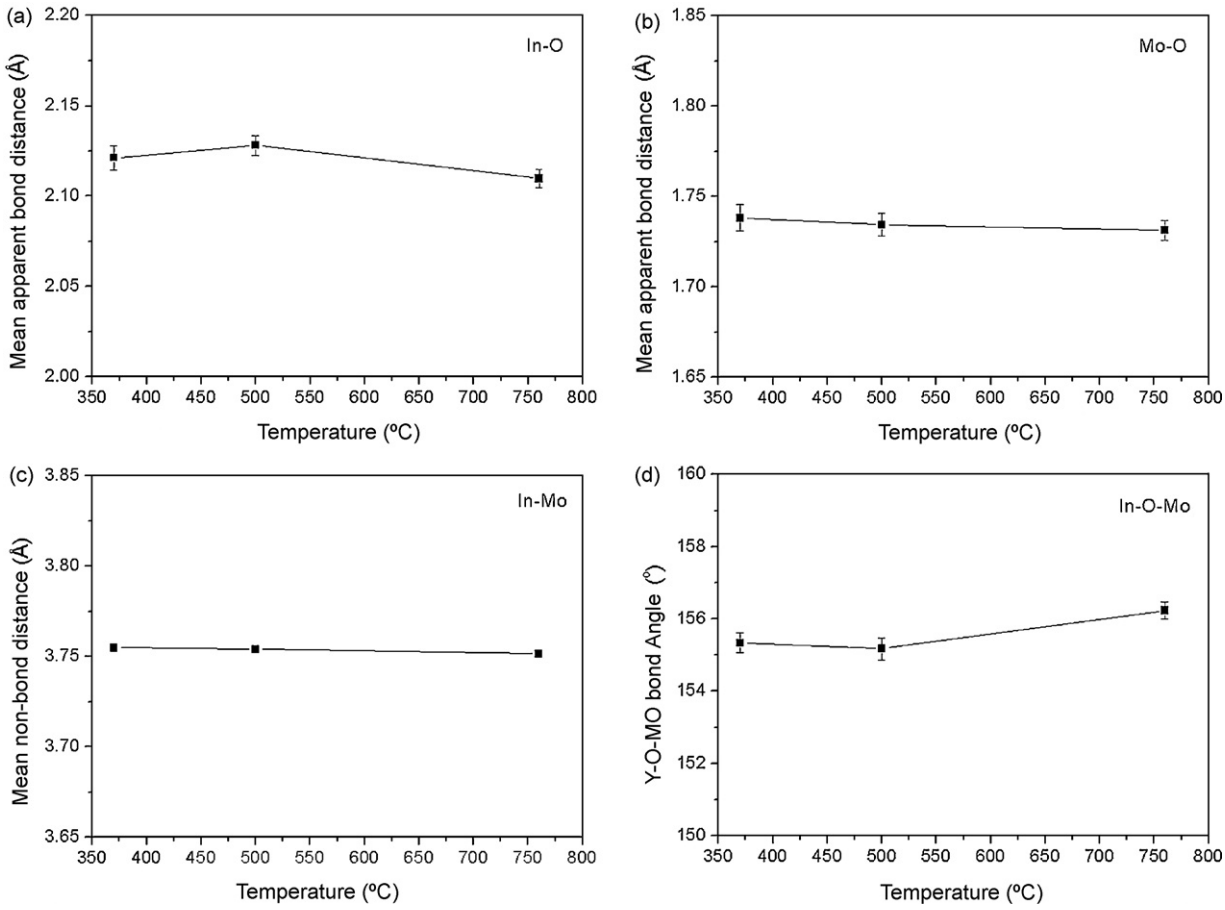

Fig. 5. Mean apparent bond distances (a) In–O and (b) Mo–O, (c) mean non-bond distances In–Mo and (d) bond angles as function of temperature.

a low negative thermal expansion, a feature that should be considered due to catalytic activity of $In_2Mo_3O_{12}$ in this temperature range. The effects of temperature (through intrinsic negative thermal expansion, dehydration and/or cation relocation) on effective size of crystal structure openings have been studied for different zeolites and other molecular sieves [23,24]. Kuznicki et al. [23] showed, for example, that pore openings in titanium silicate ETS-4 can be adjusted by temperature in order to perform selective adsorption of different gases. In another study that considered the effect of NTE on catalytic properties of zeolites, Bull et al. [24] concluded that in a silicious zeolite, called ferrierite, intercrystalline channel dimensions were hardly affected by the phenomenon of NTE.

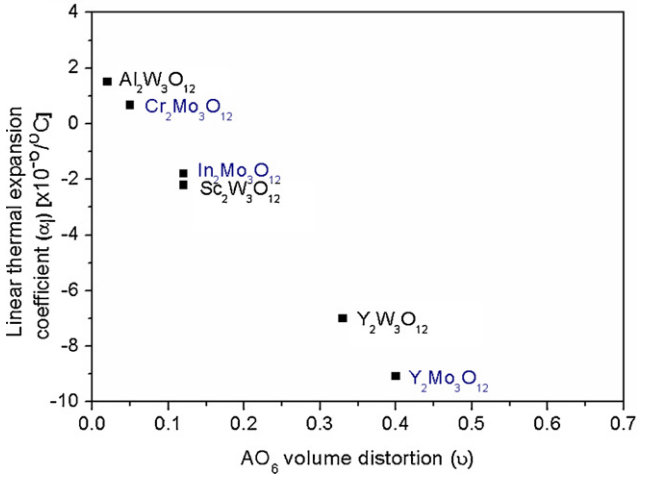

Fig. 6. Linear coefficient thermal expansion (α_l) as function of inherent AO_6 volume distortion parameter (υ) in $A_2M_3O_{12}$ family.

Based on the atomic position changes (Supplementary information) one can infer that the openings along *c* and *b* axes define the size of molecules that can pass through this structure and that these openings were almost unchanged with temperature. In order to quantify this dependence (size of the intracrystalline openings versus temperature) along *c*-axis it is useful to follow effective O1–O4 and O6–O6 distances (see Supplementary information to visualize these distances) as a function of temperature, obtained by subtracting twice the oxygen radius (1.35 Å [25]) from the distances between the centers of the anions. The O6–O6 effective distance was practically the same (~2.11 Å) over the whole temperature range, while O1–O4 even subtly increased from 1.51 Å (at 370 °C) to 1.63 Å (at 760 °C). To have insight about critical size of the openings along *b*-axis one should consider another set of O6–O6 distances which vectors form a low angle with *c*-axis (see Supplementary information to visualize this distance). The effective size of O6–O6 distances was about 2.35 Å over the studied temperature range. Taking this into account it seems that the interactions of H_2 molecules (with kinetic diameter of ~2.8 Å [25]) with $In_2Mo_3O_{12}$ do not occur within structure openings and consequently that its catalytic activity would not be affected by negative thermal expansion.

In future, thermal stability of $In_2Mo_3O_{12}$ should be evaluated under hydrogen atmosphere in order to simulate working conditions in SHC process, as previously performed by Achary et al. [26] for $Al_2W_3O_{12}$.

5. Conclusions

Monoclinic to orthorhombic phase transition in $In_2Mo_3O_{12}$ occurs around 340 °C. Monoclinic phase has normal, positive thermal expansion, while orthorhombic shows a low negative linear thermal expansion coefficient ($\alpha_l = -1.85 \times 10^{-6}\,°C^{-1}$). The linear coefficient of thermal expansion for orthorhombic $In_2Mo_3O_{12}$ is correlated with inherent volume distortion parameter (υ) of InO_6 as previously proposed [8] illustrating robustness of this new relationship. It can be inferred that thermal expansion properties in $A_2M_3O_{12}$ can be directly related to the distortion level of AO_6 polyhedra. Another important feature of AO_6 polyhedra, including InO_6, is that their distortion increases as a function of temperature.

Orthorhombic $In_2Mo_3O_{12}$ is structurally stable in air over the whole investigated temperature range (370–760 °C). The size of intercrystalline openings are almost unaffected by temperature, suggesting that hydrogen interaction with $In_2Mo_3O_{12}$ during SHC process is not sensible to NTE.

Acknowledgment

B.A.M. is grateful to the Brazilian Synchrotron Light Laboratory (LNLS) for the beam time and financial support under the project D10B-XPD 7756. R.R.A and F.R thank the fellowship from CNPq. M.A. thanks FAPERJ for postdoctoral fellowship.

Appendix A. Supplementary data

Supplementary data associated with this article can be found, in the online version, at doi:10.1016/j.tca.2009.10.021.

References

[1] J.G. Tsikoyiannis, D.L. Stern, R.K. Grasselli, J. Catal. 184 (1999) 77–86.
[2] A.W. Sleight, L.H. Brixner, J. Solid State Chem. 7 (1973) 172–174.
[3] T. Varga, J.L. Moats, S.V. Ushakov, A. Navorotsky, J. Mater. Res. 22 (2007) 2512–2521.
[4] J.S.O. Evans, T.A. Mary, A.W. Sleight, J. Solid State Chem. 133 (1997) 580–583.
[5] M. Ari, P.M. Jardim, B.A. Marinkovic, F. Rizzo, F.F. Ferreira, J. Solid State Chem. 181 (2008) 1472–1479.
[6] B.A. Marinkovic, P.M. Jardim, R.R. de Avillez, F. Rizzo, Solid State Sci. 7 (2005) 1377–1383.
[7] B.A. Marinkovic, P.M. Jardim, M. Ari, R.R. de Avillez, F. Rizzo, F.F. Ferreira, Phys. Stat. Sol. B 245 (2008) 2514–2519.
[8] B.A. Marinkovic, M. Ari, R.R. de Avillez, F. Rizzo, F.F. Ferreira, K.J. Miller, M.B. Johnson, M.A. White, Chem. Mater. 21 (2009) 2886–2894.
[9] E. Makovicky, T. Balic-Zunic, Acta Cryst. B 54 (1998) 766–773.
[10] M.M. Wu, Y.Z. Cheng, J. Peng, X.L. Xiao, D.F. Chen, R. Kiyanagi, J.S. Fieramosca, S. Short, J. Jorgensen, Z.B. Hu, Mater. Res. Bull. 42 (2007) 2090–2098.
[11] J. Peng, M.M. Wu, H. Wang, Y.M. Hao, Z. Hu, Z.X. Yu, D.F. Chen, R. Kiyanagi, J.S. Fieramosca, S. Short, J. Jorgensen, J. Alloys Compd. 453 (2008) 49–54.
[12] Z.X. Yu, J. Peng, H. Wang, M.M. Wu, Y.Z. Cheng, Z.B. Hu, D.F. Chen, Sci. China Ser. E—Tech. Sci. 51 (2008) 25–32.
[13] M.M. Wu, X.L. Xiao, Z.B. Hu, Y.T. Liu, D.F. Chen, Solid State Sci. 11 (2009) 325–329.
[14] P.M. Forster, A. Yokochi, A.W. Sleight, J. Solid State Chem. 140 (1998) 157–158.
[15] J.S.O. Evans, T.A. Mary, Inter. J. Inorg. Mater. 2 (2000) 143–151.
[16] X.L. Xiao, Y.Z. Cheng, J. Peng, M.M. Wu, D.F. Chen, Z.B. Hu, R. Kiyanagi, J.S. Fieramosca, S. Short, J. Jorgensen, Solid State Sci. 10 (2008) 321–325.
[17] F.F. Ferreira, E. Granado, W. Carvalho Jr., S.W. Kycia, D. Bruno, R. Droppa Jr., J. Synchrotron Rad. 13 (2006) 46–53.
[18] W.M. Yim, R.J. Paff, J. Appl. Phys. 45 (1974) 1456–1457.
[19] A.A. Coelho, Topas – Academic, Technical Reference, 2004.
[20] B.H. Toby, Powder Diff. 21 (2006) 67–70.
[21] J.S.O. Evans, T.A. Mary, A.W. Sleight, J. Solid State Chem. 120 (1995) 101–104.
[22] P.M. Forster, A.W. Sleight, Inter. J. Inorg. Mater. 1 (1999) 123–127.
[23] S.M. Kuznicki, V.A. Bell, S. Nair, H.W. Hillhouse, R.M. Jacubinas, C.M. Braunbarth, B.H. Toby, M. Tsapatsis, Nature 412 (2001) 720–724.
[24] I. Bull, P. Lightfoot, L.A. Villaescusa, L.M. Bull, R.K.B. Gover, J.S.O. Evans, R.E. Morris, J. Am. Chem. Soc. 125 (2003) 4342–4349.
[25] D.W. Breck, Zeolite Molecular Sieves, Wiley, New York, 1974.
[26] S.N. Achary, S. Varma, A.K. Tyagi, J. Physics. Chem. Solid 66 (2005) 1200–1205.